Bioorganic & Medicinal Chemistry 21 (2013) 2663–2670

Contents lists available at SciVerse ScienceDirect

Bioorganic & Medicinal Chemistry

journal homepage: www.elsevier.com/locate/bmc

Novel indoline-2,3-dione derivatives as inhibitors of aminopeptidase N (APN)

Kang Jin, Xiaopan Zhang, Chunhua Ma, Yingying Xu, Yumei Yuan, Wenfang Xu *

Department of Medicinal Chemistry, School of Pharmacy, Shandong University, 44, West Culture Road, Jinan, Shandong 250012, China

ARTICLE INFO

Article history:
Received 8 May 2012
Revised 12 June 2012
Accepted 13 June 2012
Available online 19 June 2012

Keywords:
Aminopeptidase N
Inhibitors
Indoline-2,3-dione derivatives
Synthesis
QSAR

ABSTRACT

Aminopeptidase N (APN/CD13), as a zinc-containing ectoenzyme, plays a critical role in the process of tumor angiogenesis, invasion and metastasis. Through the docking-based virtual screening of chemical databases and the further activity assay, we discovered that compound **10c** exhibits potent and selective inhibitory ability towards APN. In addition, a series of indoline-2,3-dione derivates have been designed and synthesized as APN inhibitors. The results of preliminary activity evaluation showed that compound **12a** (IC_{50} = 0.074 ± 0.0026 μM) exhibited the best inhibitory activity against APN, which could be used for further anticancer agent research.

1. Introduction

Aminopeptidase N (APN/CD13) is a zinc-dependent metalloprotease which is located on cell surface as an ectoenzyme.[1] It is a ubiquitous enzyme, which is widely expressed on hematopoietic cells of myeloid origin and non-hematopoietic cells and tissues, such as brain cells, fibroblasts, and epithelial cells of the kidney, liver, and intestine.[2–5] It has been certified that the over-expression of APN is associated with many diseases, such as cancer, viral infection and inflammation. Especially in the process of tumorigenesis, it played a crucial role in tumor invasion, metastasis and angiogenesis.[1,6,7]

Since the first marketed anti-APN drug Bestatin has been launched in 1976, a lot of APN inhibitors (APNIs) have been reported, for example, probestin,[8] lapstatin,[9] AHPA-Val,[10] etc. have displayed efficient inhibitory ability. Through the previous research of the structure–activity relationship (SAR) of many APNIs, it is obvious that a zinc binding group (ZBG), two hydrophobic groups and an appropriate group which can occupy the S_2' pocket are usually necessary.[11–13] Based on the brief analysis of the characteristic of the structures of the active site and inhibitors, we carried out the virtual screening and obtained 24 qualified compounds. Though the further enzyme inhibition assay, compound **10c** exhibited the best inhibitory activity against APN, which is better than Bestatin as well. Based on this, a series of APNIs had been designed (Fig. 1). And these previous work were in the process of submission now. In this letter, we described the synthesis and biological activity evaluation of these APNIs which derived from compound **10c**. The docking studies of the interaction were also discussed.

2. Chemistry

The target compounds were synthesized efficiently following the procedures shown in Schemes 1 and 2. Compounds **3a**–**3e** were easily prepared from substituted anilines **1a**–**1e** through Sandmeyer reaction. First, substituted anilines reacted with hydroxylamine hydrochloride and chloral hydrate to give nitroso acetanilides **2a**–**2e**. Then the compounds **2a**–**2e** were cyclized under the effect of concentrated sulfuric acid and hydrolyzed in the ice water to afford substituted isatins **3a**–**3e**. The compounds **4a**–**4e** were synthesized by condensation of the ketone group of compounds **3a**–**3e** and ethane-1,2-diol under acidic environment. Using different reactant, such as propane-1,3-diol and butane-1,4-diol, compounds **5a**–**5e** and **6a**–**6c** were obtained through the same method. Coupled compounds **4a**–**4e** with methyl 2-bromoacetate to get compounds **7a**–**7e**, which reacted with NH_2OK in methanol to generate the target compounds **10a**–**10e**. Compounds **11a**–**11e** and **12a**–**12c** were obtained via the same procedure.

Compound **7c** was hydrolyzed by KOH/H_2O in ethanol to obtain compound **13**, which was coupled with different natural α-amino acids to get compounds **14a**–**14f**. Finally, compounds **15a**–**15f** were obtained by treating compounds **14a**–**14f** with NH_2OK in methanol.

* Corresponding author. Tel./fax: +86 531 88382264.
E-mail address: wfxu@yahoo.cn (W. Xu).

0968-0896/$ - see front matter © 2012 Published by Elsevier Ltd.
http://dx.doi.org/10.1016/j.bmc.2012.06.024

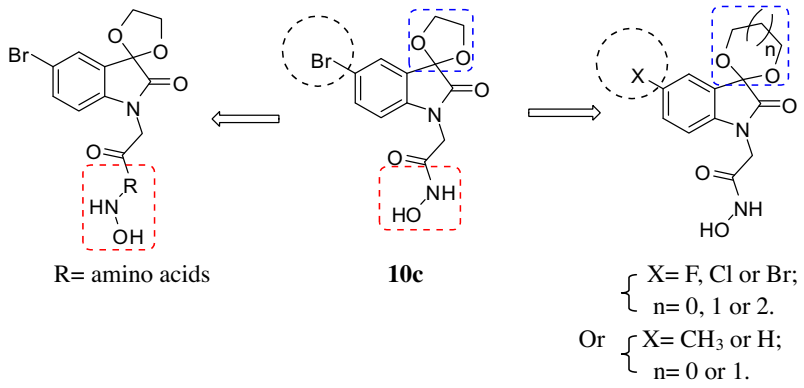

Figure 1. The new APNIs derived from compound **10c**.

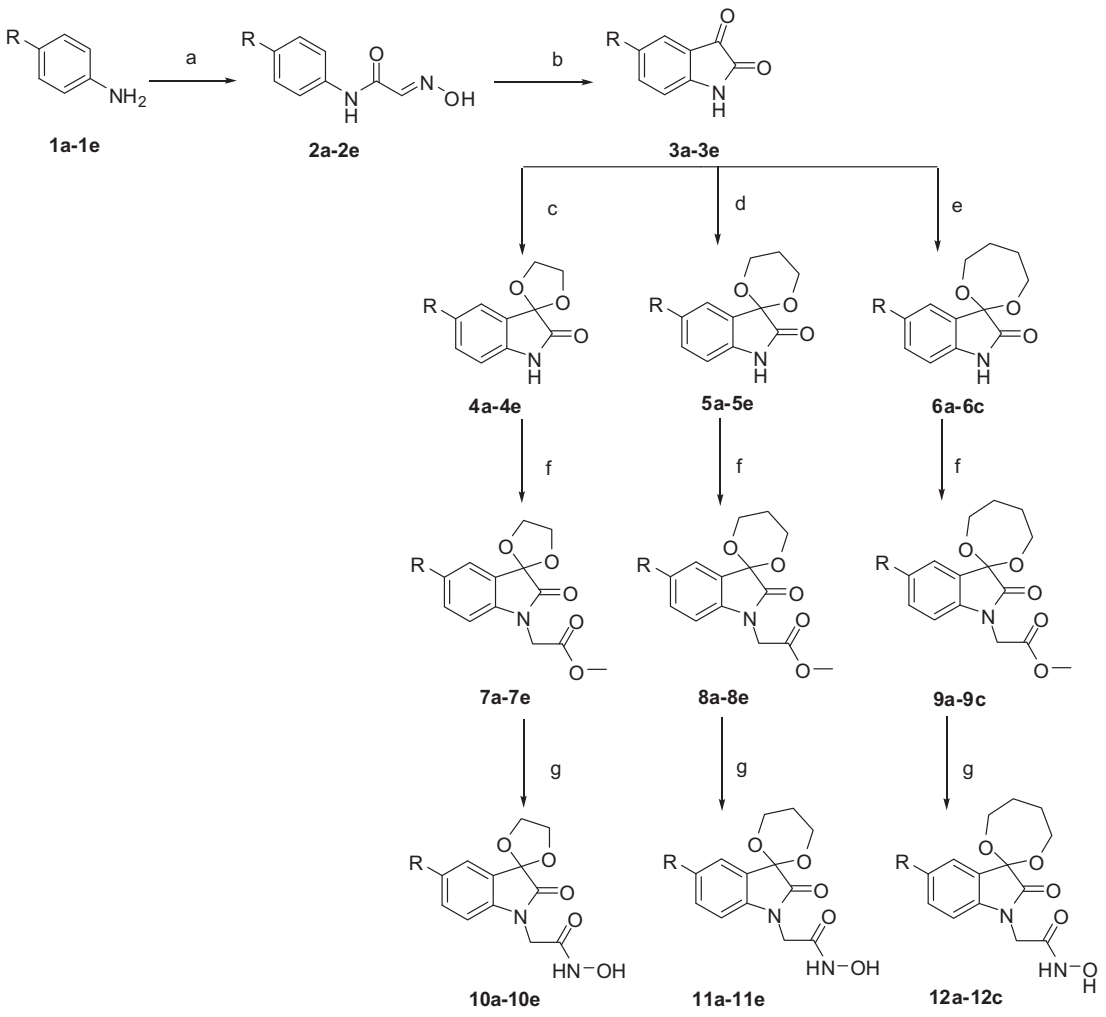

Scheme 1. Reagents and conditions: (a) $Cl_3CH(OH)_2$, NH_2OH, Na_2SO_4, 85 °C; (b) H_2SO_4, 90 °C; (c) ethane-1,2-diol, TsOH, toluene, 130 °C; (d) propane-1,3-diol, TsOH, toluene, 130 °C; (e) butane-1,4-diol, TsOH, toluene, 130 °C; (f) $BrCH_2COOCH_3$, TBAB, K_2CO_3, KI, acetone, 60 °C; (g) NH_2OK, CH_3OH.

3. Results and discussion

All the target compounds were assayed for their potential APN inhibitory activities and the results are listed in Tables 1 and 2. As the data shown, the compounds of Table 1 exhibited better inhibitory activity than the other compounds in Table 2, which suggested that the side chain which contains a hydroxamate group should have a certain length. Compared with compound **15a**, **10c** showed a better potency, which also convincingly demonstrated that the extension of side chain could trigger a reducing of the activity.

From the data of Table 1, we can see that compounds **10d** and **11d** displayed worse activities than the other ones listed in the same form, which means a substituent in R position such as chlorine, fluorine, bromine, or methane could enhance the potency of inhibitors. And different halogens in R position also have different

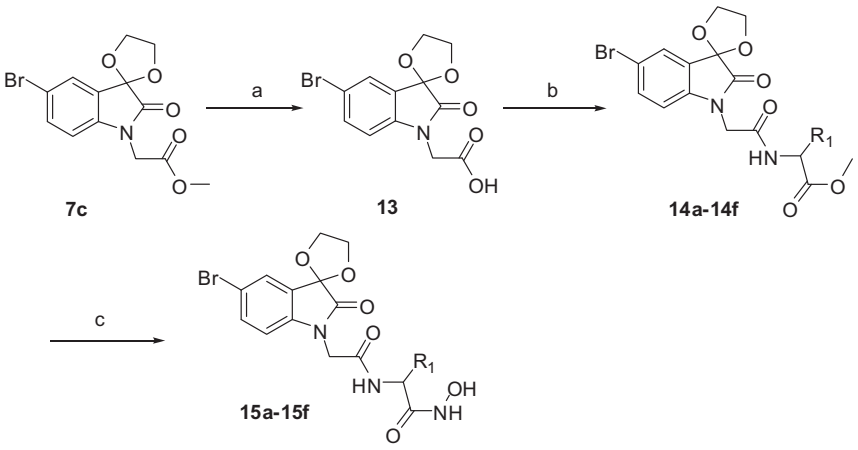

Scheme 2. Reagents and conditions: (a) EtOH, KOH, HCl; (b) methyl ester of amino acids, isobutyl chloroformate, NMM, THF, −20 °C; (c) NH_2OK, CH_3OH.

levels of impacts on their activities. The compounds with a chloride group on the benzene ring (**10a**, **11a** and **12a**) were more potent than others containing a bromide substituent (**10c**, **11c** and **12c**), followed by the fluorinate inhibitors (**10b**, **11b** and **12b**) at last. This may be a result of different influent effects of electrical properties and spatial structures of these subgroups. For example, the negative inductive effect of fluorine is stronger than chlorine and bromide, which makes the π-electron density on the benzene ring reduce. As a result, compared with the chlorinated and brominated ones, the π–π interaction between fluorinated compounds and Tyr[376] of APN weakened. On the other hand, the ability of electronic-supplying conjugation of chlorine is a little better than bromine, which made the interaction stronger as result. Besides halogens, alkyl group in R position could also affect the inhibitory ability positively. For example, compounds **10e** and **11e** with a methyl group in respective structure showed better IC_{50} values than **10d** and **11d** but worse than Bestatin and the derivatives with chlorine and bromide. So the further transformation of the structures of **10** and **11** was not continued.

On the other hand, compounds possessing ketal spiro five- to seven-membered rings sat the 3-postion of indolin-2-one skeleton also exhibited varied activities. For example, seven-membered heterocyclic derivatives **12a**, **12b** and **12c** displayed the highest potency for the inhibition of APN followed by the inhibitors **10a**, **10b** and **10c** containing five-membered heterocyclic ring. Yet the six-membered heterocyclic counterpart (**11a**, **11b** and **11c**) could not perform as strongly as the above correspondent compounds. This may due to that compared with six-member ring, the conformations of seven-member and five-member rings may be more conductive to the formation of hydrophobic effect with Met[260].

According to the data of Table 2, all the amino acid derivatives (**15a**–**15f**) showed worse activity than compound **10c**, which may indicated that the addition of the amino acid residues in the side chain could affect the affinity negatively. In this series, compound **15a** containing a Gly residue in the side chain also showed an acceptable activity against the enzyme, yet compounds with other

Table 1
The structures and inhibitory activities of the target compounds **10a**–**e**, **11a**–**e** and **12a**–**c** against APN

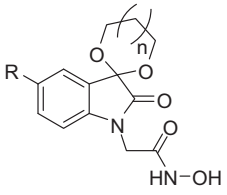

Compd	R	*n*	IC_{50}[a] (μM) APN
10a	Cl	0	0.31 ± 0.076
10b	F	0	5.30 ± 0.231
10c	Br	0	0.36 ± 0.084
10d	H	0	209.13 ± 5.32
10e	CH_3	0	2.63 ± 0.241
11a	Cl	1	1.30 ± 0.212
11b	F	1	6.71 ± 0.360
11c	Br	1	3.40 ± 0.190
11d	H	1	265.84 ± 7.13
11e	CH_3	1	3.33 ± 0.150
12a	Cl	2	0.074 ± 0.0026
12b	F	2	4.06 ± 0.357
12c	Br	2	0.086 ± 0.00201
Bestatin	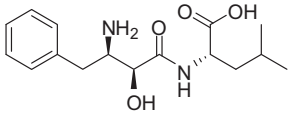		1.30 ± 0.085

[a] Mean values and standard deviations of triplicate experiments are given.

Table 2
The structures and inhibitory activities of the target compounds **15a**–**f** and positive control bestatin against APN

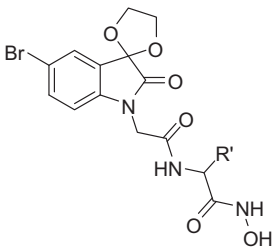

Compd	R′	IC_{50}[a] (μM) APN
15a	–H	6.60 ± 0.512
15b	$-CH_2Ph$	26.38 ± 1.86
15c	$-CH_2CH(CH_3)_2$	22.46 ± 1.54
15d	$-CH(CH_3)CH_2CH_3$	631.22 ± 9.25
15e	–Ph	>1000
15f	$-CH(CH_3)_2$	226.07 ± 2.11
Bestatin	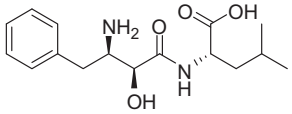	1.30 ± 0.085

[a] Mean values and standard deviations of triplicate experiments are given.

Table 3
the structures and inhibitory activities of compounds **10a–c**, **11a–c**, **12a–c** and **15a** against HDAC

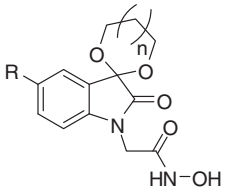

Compd	R	*n*	IC_{50}[a] (μM) HDAC
10a	Cl	0	>100
10b	F	0	>100
10c	Br	0	>100
11a	Cl	1	>100
11b	F	1	>100
11c	Br	1	>100
12a	Cl	2	>100
12b	F	2	>100
12c	Br	2	>100
15a	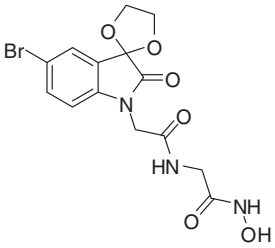		0.33 ± 0.076
SAHA	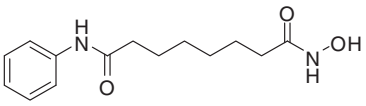		0.11 ± 0.03

[a] Mean values and standard deviations of triplicate experiments are given.

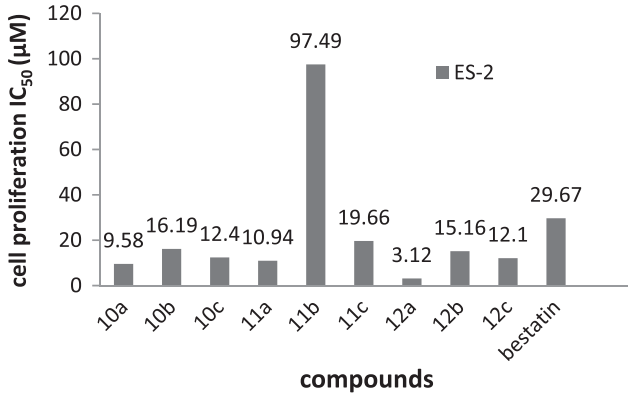

Figure 2. Inhibitory activity of compounds **10a–c**, **11a–c**, **12a–c** and Bestatin against APN on ES-2 cells. Data expressed are mean values of three independent experiments.

amino acids in the same position did not exhibit expected potency towards APN. This may be explained by that the larger hydrophobic isatin group could bind tightly with APN's S2′ active pocket, but the hydrophobic side chains of amino acids could not occupy the S1′ pocket as originally designed.

Comparing all the target compounds (compounds **10**, **11**, **12** and **15**), compound **12a** had a better inhibition (IC_{50} = 0.074 ± 0.0026 μM) than the others and control Bestatin (IC_{50} = 1.3 ± 0.085 μM).

In order to test the selectivity, compounds **10a–c**, **11a–c**, **12a–c** and **15a** which showed satisfactory activities against APN were chosen to be assayed for the inhibition of HDACs with SAHA as the positive control. HDACs are zinc-dependent metalloproteinase as well and associated closely with the invasion and metastasis of tumor. Unlike APN, which is an exopeptidase, HDACs mainly exist near nucleus. As the results shown in Table 3, all the tested compounds but **15a** exhibited much lower inhibitory activities against HDACs than that of APN, which to some verified our APNIs designing strategy. Compared with SAHA, **15a** showed a similar inhibitory ability against HDACs, the reason of which may be that **15a** could bind with the active side of HDACs by its side chain going through the slender channel, just like SAHA. Thus **15a** could be used as a leader to design more potent HDACs inhibitors in the future.

Furthermore, the inhibition of compounds **10a–c**, **11a–c** and **12a–c** against human APN were also determined with ES-2 human ovarian clear cell carcinoma cells high-expressing APN. Results were presented in Figure 2, from which we can see that all these compounds, expect for **11b**, could inhibit APN on ES-2 cells more efficiently than Bestatin, and **12a** showed the best capability (IC_{50} = 3.12 ± 0.56 μM). Similar to the above enzyme inhibitory activity, the human APN inhibition of these compounds also presented consistent trends. The chloride substituent in **R** position enhanced the potency more obviously than bromide substituent followed by fluoride ones at last (**10a** > **10c** > **10b**, **11a** > **11c** > **11b**, **12a** > **12c** > **12b**). The same rule as the results of previous enzymatic inhibition experiment also appeared from the perspective of these compounds with different heterocyclic rings (**12a** > **10a** > **11a**, **12b** > **10b** > **11b**, **12c** > **10c** > **11c**).

In addition, we also selected compounds **10a–c**, **11a–c** and **12a–c** to assay their anti-tumor inhibitory activity against ES-2 cell proliferation compared with Bestatin by using MTT method. The results confirmed that the anti-tumor inhibitory activities of compounds (**10a** IC_{50} = 167.19 ± 21.47 μM, **10b** IC_{50} = 141.50 ± 11.19 μM, **10c** IC_{50} = 204.69 ± 32.33 μM, **11a** IC_{50} = 233.34 ± 18.52 μM, **11c** IC_{50} = 137.14 ± 15.21 μM, **12a** IC_{50} = 212.25 ± 17.84 μM) are similar to each other and all of these compounds exhibited better anti-proliferative effect against ES-2 cells than Bestation with the IC_{50} of 631.74 ± 29.70 μM (Fig. 3). The assay of **10a–c**, **11a–c** and **12a–c** on MDA-MB-231 cell proliferation was also performed, the results of which were shown in Figure 4. Compounds **10c**, **11c**, **12a** and **12c** exhibited the inhibitory effect with IC_{50} values of 57.45 ± 10.21 μM, 55.12 ± 6.83 μM, 91.52 ± 15.82 μM and 32.85 ± 5.32 μM, which showed similar potency to Bestatin with IC_{50} value of 50.6 ± 4.68 μM.

Aiming to investigate the interaction between the target compounds and APN, the most active compound **12a**, was chosen to be constructed using a Sybyl/Sketch module and optimized via

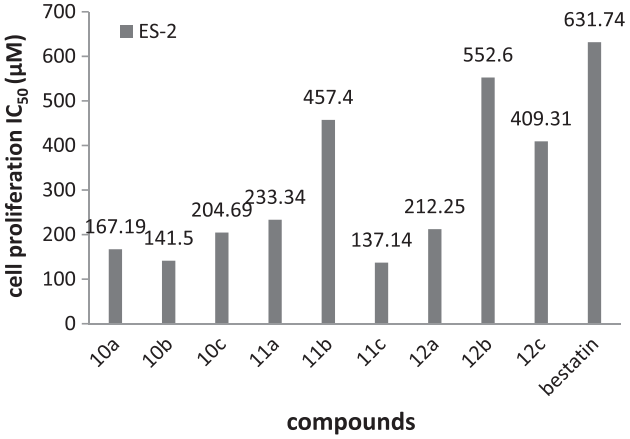

Figure 3. Effects of compounds **10a–c**, **11a–c**, **12a–c** and Bestatin on ES-2 cells proliferation. The columns represent the mean values of three independent experiments.

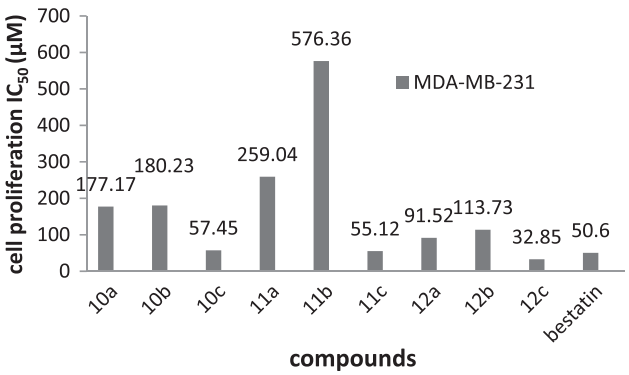

Figure 4. Effects of compounds **10a–c**, **11a–c**, **12a–c** and Bestatin on MDA-MB-231 cells proliferation. The columns represent the mean values of three independent experiments.

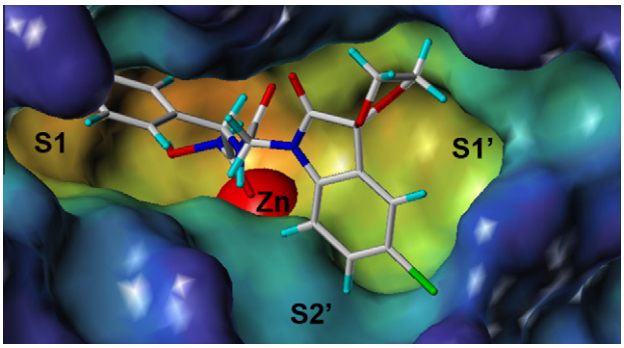

Figure 6. The docking result of compound **15e** with APN.

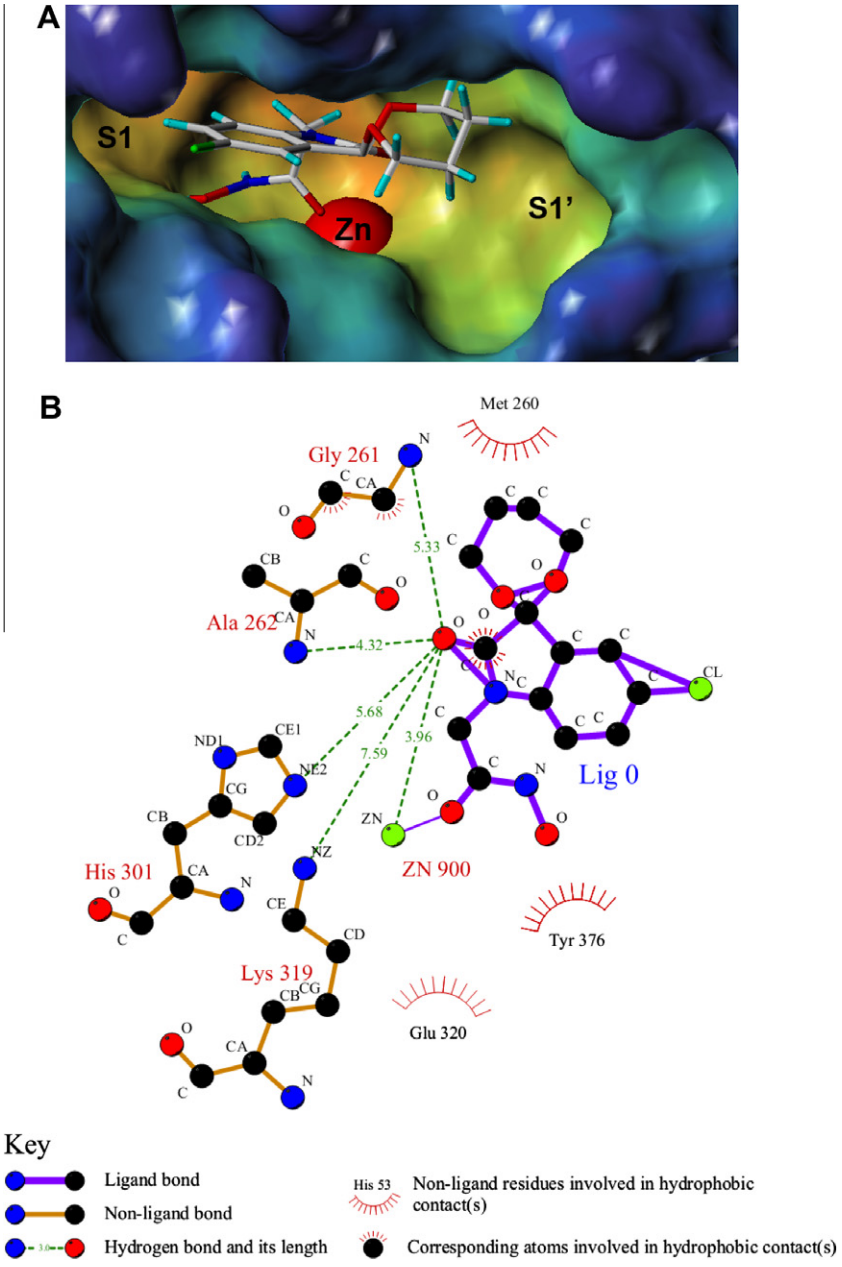

Figure 5. (a) The FlexX docking result of **12a** with APN (PDB: 2DQM). (b) The docking result of **12h** shown by LIGPLOT.

Powell's method by the Tripos force field with convergence criterion set at 0.05 kcal/(Å mol), and assigned with the Gasteiger–Hückel method. The docking study of **12a** and the active site of APN was performed using Sybyl/FlexX module. The active site was defined as 7.0 Å radius circles around Bestatin in the co-crystal structure (PDB code: 2DQM). Other docking parameters utilized in the program were remained default. The result showed in Figure 5a suggested that the large hydrophobic backbone of 5′-chlorospiro[[1,3]dioxepane-2,3′-indolin]-2′-one can insert into S1 pocket and the hydroxamic acid group can chelate with the zinc ion which was the crucial catalytic factor in active site. In addition, a 2D pattern of detailed binding mode was created as well (Fig. 5b). The large isatin moiety of compound **12a** can form hydrophobic interaction with Met^{260}, Tyr^{376} and Glu^{320} of S1 pocket and the carbonyl group can from hydrogen bonds with Gly^{261}, Ala^{262}, His^{301}, Lys^{319} and the zinc ion at the distance of 5.33, 4.32, 5.68, 7.59 and 3.96 Å, respectively. The compounds with less activities showed in Table 2, may have a different interaction modes. In order to investigate the causing of the decline in activity, compound **15e** was selected for docking study by the same method with compound **12a**. As illustrated in Figure 6, the phenyl group of L-phenylglycine moiety can slightly interact with S1 pocket with an unsatisfactory angle. Although the hydroxamic acid group can also chelate the zinc ion, the lager hydrophobic 5′-bromospiro[[1,3]dioxolane-2,3′-indolin]-2′-one moiety cannot insert into S2′ pocket, so compound **15e** had a less inhibitory activity than **12a**.

4. Conclusion

In summary, the synthesis and properties of one series of indoline-2,3-dione derivates as APNIs have been described. The preliminary results demonstrated that most of the target compounds exhibited better inhibition than the control Bestatin. Comparing with the lead compound **10c**, the inhibitory activities toward APN were also improved mildly. Among them, compound **12a** showed the most effective inhibition, which could be used as a lead for further structure transformation in the future APNIs exploration.

5. Experiment

5.1. Chemistry: general procedures

All the materials involved were purchased from commercial suppliers. Solvents were distilled prior to use. All the reactions were monitored by thin-layer chromatography on 0.25 mm silica gel plates (60GF-254) and visualized with UV light, or chloride ferric. The products were purified by column chromatography which was performed using 200–300 mesh silica gel. NMR spectra were determined on a Brucker Avance 600 spectrometer, δ in parts per million and J in Hertz. TMS was used as an internal standard. ESI-MS were determined on an API 4000 spectrometer. Measurements were made in DMSO-d_6 solutions. Melting points were tested using an electrothermal melting point apparatus and were uncorrected.

5.1.1. *N*-(4-Fluorophenyl)-2-(hydroxyimino) acetamide (2a)

Anhydrous sodium fulfate (120 g, 0.84 mol) was dissolved in lukewarm water (350 mL) and an aqueous solution of chloral hydrate (14.89 g, 0.09 mol, 30 mL) was added to the solution. A mixture of compound **1a** (7.65 g, 0.06 mol), concentrated hydrochloric acid (15 mL) and distilled water (105 mL) was added dropwise to the solution. Then an aqueous solution of hydroxylamine hydrochloride (13.9 g, 0.20 mol, 60 mL) was added and the reaction mixture was stirred for 2 h at 85 °C. Then cool the mixture to room temperature and brown solid was precipitated to give crude product *N*-(4-fluorophenyl)-2-(hydroxyimino) acetamide. The crude product was recrystallized by distilled water to give compound **2a** as white solid (10.18 g, yield 85.4%), mp = 173–175 °C.

5.1.2. 5-Chloroindoline-2,3-dione (3a)

Compound **2a** (9.93 g, 0.05 mol) was added to concentrated sulfuric acid (40 mL) in batches at 60 °C. Keep the reaction at 90 °C for 30 min. Cool the mixture to room temperature and then pour the solution into ice-water (200 mL) with vigorous stirring for 1 h. Orange solid was precipitated as crude product, which was depurated by column chromatography to get compound **3a** (8.18 g, yield 90.1%), mp = 237–239 °C.

5.1.3. 5′-Chlorospiro[[1,3]dioxolane-2,3′-indolin]-2′-one (4a)

A solution of compound **3a** (1.00 g, 6.21 mmol), ethylene glycol (2.3 g, 31.05 mmol) and TsOH (1.07 g, 6.21 mmol) in 150 mL toluene was stirred for 5 h at 130 °C. The water which was produced in the reaction system was removed by water separator frequently. The toluene was removed with a rotary evaporator. The remaining mixture was dissolved in 50 mL EtOAc and washed with saturated $NaHCO_3$ (10 mL × 3) and brine (10 mL × 2) in turn. The organic phase was dried over anhydrous $MgSO_4$, filtered and concentrated with a rotary evaporator to give the crude product. The crude product was depurated by column chromatography to afford compound **4a** as white solid (0.97 g, yield: 78.2%), mp = 178–179 °C. ^{1}H NMR (600 MHz, DMSO) δ 10.60 (s, 1H), 7.43 (d, J = 2.2 Hz, 1H), 7.39 (dd, J = 8.3, 2.2 Hz, 1H), 6.85 (d, J = 8.3 Hz, 1H), 4.34–4.25 (m, 4H). ESI-MS m/z: 226.6 $[M+1]^+$.

5.1.4. Methyl-2-(5′-chloro-2′-oxospiro[[1,3]dioxolane-2,3′-indoline]-1′-yl)acetate (7a)

To a solution of compound **4a** (0.5 g, 2.2 mmol) and methyl-2-bromoacetate (0.4 g, 2.64 mmol) in 50 mL acetone was added TBAB (0.07 g, 0.22 mmol) and KI (0.036 g, 0.22 mmol) as catalyst. Then K_2CO_3 (0.36 g, 2.64 mmol) was added to the reaction mixture. Keep the reaction for 6 h at 56 °C. Filtrated and concentrated in vacuum. The residue was dissolved in 50 mL EtOAc and washed with saturated $NaHCO_3$ (10 mL × 3) and brine (10 mL × 2) in turn. The EtOAc solution was dried over anhydrous $MgSO_4$ and concentrated with a rotary evaporator to get the crude product. The crude product was purified by fast column chromatograph (PE/EtOAc = 10:1) to afford compound **7a** as white solid (0.62 g, yield: 95.4%), mp = 123–124 °C. ^{1}H NMR (600 MHz, DMSO) δ 7.53 (d, J = 2.0 Hz, 1H), 7.49 (dd, J = 8.4, 2.1 Hz, 1H), 7.11 (d, J = 8.4 Hz, 1H), 4.55 (s, 2H), 4.37–4.29 (m, 4H), 3.68 (s, 3H). ESI-MS m/z: 298.4 $[M+1]^+$.

5.1.5. 2-(5′-Chloro-2′-oxospiro[[1,3]dioxolane-2,3′-indoline]-1′-yl)-*N*-hydroxyacetamide (10a)

Compound **7a** (0.5 g, 1.68 mmol) was dissolved to a solution of 1.5 N NH_2–OK in methanol (10 mL). The reaction mixture was stirred for 1.5 h, and then concentrated in vacuum to give the yellow oily liquid. The residue was acidified by 1 N HCl and extracted with ethyl acetate. The organic phase was dried with Na_2SO_4, and then remove the solvent under low pressure to get the crude product. Finally, compound **10a** was separated by column chromatography (PE/EtOAc = 1:1) as white solid (0.34 g, yield: 68.0%), mp = 165–166 °C. ^{1}H NMR (600 MHz, DMSO) δ 10.87 (s, 1H), 9.04 (s, 1H), 7.52–7.48 (m, 2H), 7.01–6.97 (m, 1H), 4.34–4.31 (m, 4H), 4.20 (s, 2H). HRMS (AP-ESI) m/z Calcd for $C_{12}H_{11}ClN_2O_5$ $[M+H]^+$ 299.0356. Found: 299.0426.

The other compounds (**10b**–**10e**, **11a**–**11e**, **12a**–**12c**) were synthesized by the same method.

5.1.6. 2-(5′-Fluoro-2′-oxospiro[[1,3]dioxolane-2,3′-indoline]-1′-yl)-*N*-hydroxyacetamide (10b)

White solid, yield 73.1%, mp = 175–176 °C. ^{1}H NMR (600 MHz, DMSO) δ 10.87 (s, 1H), 9.03 (s, 1H), 7.34 (dd, J = 7.6, 2.5 Hz, 1H),

7.29 (td, J = 9.1, 2.5 Hz, 1H), 6.97 (dd, J = 8.6, 4.0 Hz, 1H), 4.36–4.33 (m, 2H), 4.30 (dd, J = 8.4, 4.0 Hz, 2H), 4.19 (s, 2H). HRMS (AP-ESI) m/z Calcd for $C_{12}H_{11}FN_2O_5$ $[M+H]^+$ 283.0652. Found: 283.0719.

5.1.7. 2-(5′-Bromo-2′-oxospiro[[1,3]dioxolane-2,3′-indoline]-1′-yl)-*N*-hydroxyacetamide (10c)

White solid, yield 72.3%, mp = 163–164 °C. ^{1}H NMR (600 MHz, DMSO) δ 10.87 (s, 1H), 9.03 (s, 1H), 7.63 (dd, J = 8.4, 2.0 Hz, 1H), 7.60 (d, J = 1.9 Hz, 1H), 6.94 (d, J = 8.4 Hz, 1H), 4.34–4.32 (m, 2H), 4.32–4.30 (m, 2H), 4.19 (s, 2H). HRMS (AP-ESI) m/z Calcd for $C_{12}H_{11}BrN_2O_5$ $[M+H]^+$ 342.9851. Found: 342.9928.

5.1.8. *N*-Hydroxy-2-(2′-oxospiro[[1,3]dioxolane-2,3′-indoline]-1′-yl)acetamide (10d)

White solid, yield 69.7%, mp = 143–144 °C. ^{1}H NMR (600 MHz, DMSO) δ 10.88 (s, 1H), 9.03 (s, 1H), 7.44–7.35 (m, 2H), 7.12–7.07 (m, 1H), 6.94 (d, J = 7.9 Hz, 1H), 4.36 (d, J = 3.4 Hz, 2H), 4.29 (d, J = 3.4 Hz, 2H), 4.18 (s, 2H). HRMS (AP-ESI) m/z Calcd for $C_{12}H_{12}N_2O_5$ $[M+H]^+$ 265.0746. Found: 265.0817.

5.1.9. *N*-Hydroxy-2-(5′-methyl-2′-oxospiro[[1,3]dioxolane-2,3′-indoline]-1′-yl)acetamide (10e)

White solid, yield 75.8%, mp = 157–158 °C. ^{1}H NMR (600 MHz, DMSO) δ 10.85 (s, 1H), 9.01 (s, 1H), 7.21 (d, J = 6.2 Hz, 2H), 6.83 (d, J = 8.5 Hz, 1H), 4.36–4.34 (m, 2H), 4.29–4.26 (m, 2H), 4.14 (s, 2H), 2.28 (s, 3H). HRMS (AP-ESI) m/z Calcd for $C_{13}H_{14}N_2O_5$ $[M+H]^+$ 279.0903. Found: 279.0981.

5.1.10. 2-(5′-Chloro-2′-oxospiro[[1,3]dioxane-2,3′-indoline]-1′-yl)-*N*-hydroxyacetamide (11a)

White solid, yield 83.5%, mp = 152–153 °C. ^{1}H NMR (600 MHz, DMSO) δ 10.88 (s, 1H), 9.04 (s, 1H), 7.47 (dd, J = 8.4, 2.1 Hz, 1H), 7.41 (d, J = 2.0 Hz, 1H), 6.97 (d, J = 8.4 Hz, 1H), 4.71 (dd, J = 11.7, 9.4 Hz, 2H), 4.21 (s, 2H), 3.94 (dd, J = 11.5, 3.0 Hz, 2H), 2.23–2.12 (m, 1H), 1.69 (d, J = 13.5 Hz, 1H). HRMS (AP-ESI) m/z Calcd for $C_{13}H_{13}ClN_2O_5$ $[M+H]^+$ 313.0513. Found: 313.0586.

5.1.11. 2-(5′-Fluoro-2′-oxospiro[[1,3]dioxane-2,3′-indoline]-1′-yl)-*N*-hydroxyacetamide (11b)

White solid, yield 78.4%, mp = 161–161.5 °C. ^{1}H NMR (600 MHz, DMSO) δ 10.88 (s, 1H), 9.04 (s, 1H), 7.28–7.22 (m, 2H), 6.95 (dd, J = 8.4, 4.0 Hz, 1H), 4.72 (t, J = 10.6 Hz, 2H), 4.20 (s, 2H), 3.99–3.87 (m, 2H), 2.18 (qd, J = 12.1, 5.8 Hz, 1H), 1.69 (d, J = 13.5 Hz, 1H). HRMS (AP-ESI) m/z Calcd for $C_{13}H_{13}FN_2O_5$ $[M+H]^+$ 297.0808. Found: 297.0884.

5.1.12. 2-(5′-Bromo-2′-oxospiro[[1,3]dioxane-2,3′-indoline]-1′-yl)-*N*-hydroxyacetamide (11c)

White solid, yield 83.2%, mp = 149–150 °C. ^{1}H NMR (600 MHz, DMSO) δ 10.87 (s, 1H), 9.04 (s, 1H), 7.59 (dd, J = 8.4, 2.0 Hz, 1H), 7.51 (d, J = 2.0 Hz, 1H), 6.92 (d, J = 8.4 Hz, 1H), 4.71 (t, J = 10.6 Hz, 2H), 4.20 (s, 2H), 3.94 (d, J = 11.6 Hz, 2H), 2.23–2.11 (m, 1H), 1.69 (d, J = 13.2 Hz, 1H). HRMS (AP-ESI) m/z Calcd for $C_{13}H_{13}BrN_2O_5$ $[M+H]^+$ 357.0008. Found: 357.0081.

5.1.13. *N*-Hydroxy-2-(2′-oxospiro[[1,3]dioxane-2,3′-indoline]-1′-yl)acetamide (11d)

White solid, yield 65.6%, mp = 149–150 °C. ^{1}H NMR (600 MHz, DMSO) δ 10.88 (s, 1H), 9.03 (s, 1H), 7.37 (d, J = 7.3 Hz, 2H), 7.06 (t, J = 7.3 Hz, 1H), 6.92 (d, J = 7.8 Hz, 1H), 4.75 (td, J = 11.8, 2.6 Hz, 2H), 4.19 (s, 2H), 3.92 (dd, J = 10.8, 4.1 Hz, 2H), 2.17 (qd, J = 12.2, 6.1 Hz, 1H), 1.68 (d, J = 13.5 Hz, 1H). HRMS (AP-ESI) m/z Calcd for $C_{13}H_{14}N_2O_5$ $[M+H]^+$ 279.0903. Found: 279.0975.

5.1.14. *N*-Hydroxy-2-(5′-methyl-2′-oxospiro[[1,3]dioxane-2,3′-indoline]-1′-yl)acetamide (11e)

White solid, yield 64.1%, mp = 145–146 °C. ^{1}H NMR (600 MHz, DMSO) δ 10.85 (s, 1H), 9.02 (s, 1H), 7.20 (s, 1H), 7.16 (d, J = 8.0 Hz, 1H), 6.80 (d, J = 8.0 Hz, 1H), 4.74 (td, J = 11.7, 2.5 Hz, 2H), 4.15 (s, 2H), 3.91 (dd, J = 9.8, 5.0 Hz, 2H), 2.27 (s, 3H), 2.20–2.12 (m, 1H), 1.71–1.64 (m, 1H). HRMS (AP-ESI) m/z Calcd for $C_{14}H_{16}N_2O_5$ $[M+H]^+$ 293.1059. Found: 293.1127.

5.1.15. 2-(5′-Chloro-2′-oxospiro[[1,3]dioxepane-2,3′-indoline]-1′-yl)-*N*-hydroxyacetamide (12a)

White solid, yield 53.6%, mp = 153–154 °C. ^{1}H NMR (600 MHz, DMSO) δ 10.86 (s, 1H), 9.03 (s, 1H), 7.69 (d, J = 2.0 Hz, 1H), 7.45 (dd, J = 8.4, 2.1 Hz, 1H), 6.98 (d, J = 8.4 Hz, 1H), 4.25 (dd, J = 11.6, 4.6 Hz, 2H), 4.20 (s, 2H), 4.02 (dd, J = 10.9, 5.4 Hz, 2H), 1.71 (t, J = 8.1 Hz, 4H). HRMS (AP-ESI) m/z Calcd for $C_{14}H_{15}ClN_2O_5$ $[M+H]^+$ 327.0669. Found: 327.0745.

5.1.16. 2-(5′-Fluoro-2′-oxospiro[[1,3]dioxepane-2,3′-indoline]-1′-yl)-*N*-hydroxyacetamide (12b)

White solid, yield 48.6%, mp = 159–160 °C. ^{1}H NMR (600 MHz, DMSO) δ 10.86 (s, 1H), 9.02 (d, J = 1.2 Hz, 1H), 7.56 (dd, J = 8.1, 2.6 Hz, 1H), 7.24 (td, J = 9.2, 2.6 Hz, 1H), 6.95 (dd, J = 8.7, 4.1 Hz, 1H), 4.25 (t, J = 11.4 Hz, 2H), 4.19 (s, 2H), 4.01 (d, J = 12.1 Hz, 2H), 1.68 (d, J = 37.5 Hz, 4H). HRMS (AP-ESI) m/z Calcd for $C_{14}H_{15}FN_2O_5$ $[M+H]^+$ 311.0965. Found: 311.1038.

5.1.17. 2-(5′-Bromo-2′-oxospiro[[1,3]dioxepane-2,3′-indoline]-1′-yl)-*N*-hydroxyacetamide (12c)

White solid, yield 51.7%, mp = 152–154 °C. ^{1}H NMR (600 MHz, DMSO) δ 10.86 (s, 1H), 9.03 (s, 1H), 7.79 (d, J = 1.8 Hz, 1H), 7.58 (dd, J = 8.4, 1.9 Hz, 1H), 6.93 (d, J = 8.4 Hz, 1H), 4.24 (dd, J = 17.7, 13.2 Hz, 2H), 4.19 (s, 2H), 4.01 (dd, J = 11.1, 5.5 Hz, 2H), 1.72 (q, J = 14.0 Hz, 4H). HRMS (AP-ESI) m/z Calcd for $C_{14}H_{15}BrN_2O_5$ $[M+H]^+$ 371.0164. Found: 371.0237.

5.1.18. Methyl-2-(2-(5′-bromo-2′-oxospiro[[1,3]dioxolane-2,3′-indoline]-1′-yl)acetamido)acetate (14a)

To a solution of compound **13** (0.50 g, 1.5 mmol) and *N*-methylmorpholine (0.36 mL, 3.3 mmol) in 30 ml anhydrous THF was added isobutyl chloroformate (0.23 mL, 1.8 mmol) at −15 °C. The mixture was stirred for 30 min at the same temperature. A solution of compound glycine methyl ester hydrochloride (0.21 g, 1.65 mmol) in 20 mL THF was added dropwise to the mixture. Keep the reaction for 1 h at −15 °C, and then removed the cooling bath. The reaction mixture was stirred for another 12 h at room temperature. Filtrated and concentrated with a rotary evaporator. The residue was dissolved in 50 mL EtOAc and washed with saturated citric acid, saturated $NaHCO_3$ and brine in turn. The EtOAc phase was dried over Na_2SO_4 and concentrated with a rotary evaporator to get crude product. The crude product was purified by fast column chromatograph (PE/EtOAc = 5:1) to afford compound **14a** as white solid (0.46 g, yield: 76.7%), mp = 174–174.5 °C. ^{1}H NMR (600 MHz, DMSO) δ 7.63–7.59 (m, 2H), 6.88 (d, J = 8.1 Hz, 1H), 4.35 (s, 2H), 4.34 (d, J = 6.7 Hz, 2H), 4.31 (d, J = 3.8 Hz, 2H), 3.89 (d, J = 5.8 Hz, 2H), 3.63 (s, 3H). ESI-MS m/z: 399.2 $[M+1]^+$.

The final compounds (**15a**–**15f**) were obtained via the same method as compound **10a** which had been introduced previously.

5.1.19. 2-(5′-Bromo-2′-oxospiro[[1,3]dioxolane-2,3′-indoline]-1′-yl)-*N*-(2-(hydroxyamino)-2-oxoethyl)acetamide (15a)

White solid, yield 43.5%, mp = 173–174 °C. ^{1}H NMR (600 MHz, DMSO) δ 10.57 (s, 1H), 8.86 (d, J = 1.3 Hz, 1H), 8.57 (t, J = 5.8 Hz,

1H), 7.61–7.56 (m, 2H), 6.92–6.90 (m, 1H), 4.35–4.32 (m, 4H), 4.32–4.30 (m, 2H), 3.65 (d, J = 5.8 Hz, 2H). HRMS (AP-ESI) m/z Calcd for $C_{14}H_{14}BrN_3O_6$ $[M+H]^+$ 400.0066. Found: 400.0141.

5.1.20. 2-(2-(5′-Bromo-2′-oxospiro[[1,3]dioxolane-2,3′-indoline]-1′-yl)acetamido)-*N*-hydroxy-3-phenylpropanamide (15b)

White solid, yield 39.7%, mp = 173–174 °C. ^{1}H NMR (600 MHz, DMSO) δ 10.76 (d, J = 12.9 Hz, 1H), 8.93 (s, 1H), 8.71 (d, J = 8.7 Hz, 1H), 7.56 (d, J = 1.8 Hz, 1H), 7.45 (dd, J = 8.3, 1.7 Hz, 1H), 7.30 (t, J = 7.2 Hz, 2H), 7.25 (t, J = 7.8 Hz, 4H), 6.38 (d, J = 8.4 Hz, 1H), 4.42–4.35 (m, 2H), 4.34–4.26 (m, 4H), 3.00 (dd, J = 13.6, 5.0 Hz, 1H), 2.77 (dd, J = 13.5, 9.8 Hz, 1H). HRMS (AP-ESI) m/z Calcd for $C_{21}H_{20}BrN_3O_6$ $[M+H]^+$ 490.0535. Found: 490.0607.

5.1.21. 2-(2-(5′-Bromo-2′-oxospiro[[1,3]dioxolane-2,3′-indoline]-1′-yl)acetamido)-*N*-hydroxy-4-methylpentanamide (15c)

White solid, yield 38.9%, mp = 170–171 °C. ^{1}H NMR (600 MHz, DMSO) δ 10.73 (d, J = 1.4 Hz, 1H), 8.87 (d, J = 1.6 Hz, 1H), 8.50 (d, J = 8.3 Hz, 1H), 7.60 (dd, J = 6.8, 2.0 Hz, 2H), 6.86–6.82 (m, 1H), 4.37–4.26 (m, 6H), 4.22–4.14 (m, 1H), 1.55 (td, J = 13.5, 6.7 Hz, 1H), 1.45 (t, J = 7.3 Hz, 2H), 0.89 (d, J = 6.6 Hz, 3H), 0.82 (d, J = 6.6 Hz, 3H). HRMS (AP-ESI) m/z Calcd for $C_{18}H_{22}BrN_3O_6$ $[M+H]^+$ 456.0692. Found: 456.0769.

5.1.22. 2-(2-(5′-Bromo-2′-oxospiro[[1,3]dioxolane-2,3′-indoline]-1′-yl)acetamido)-*N*-hydroxy-3-methylpentanamide (15d)

White solid, yield 41.2%, mp = 168–169 °C. ^{1}H NMR (600 MHz, DMSO) δ 10.70 (s, 1H), 8.90 (s, 1H), 8.47 (d, J = 9.0 Hz, 1H), 7.60 (d, J = 6.1 Hz, 2H), 6.85 (d, J = 8.8 Hz, 1H), 4.43–4.25 (m, 6H), 4.00 (dd, J = 20.9, 12.5 Hz, 1H), 1.70 (s, 1H), 1.45 (s, 1H), 1.13–1.01 (m, 1H), 0.82 (t, J = 6.9 Hz, 6H). HRMS (AP-ESI) m/z Calcd for $C_{18}H_{22}BrN_3O_6$ $[M+H]^+$ 456.0692. Found: 456.0765

5.1.23. 2-(2-(5′-Bromo-2′-oxospiro[[1,3]dioxolane-2,3′-indoline]-1′-yl)acetamido)-*N*-hydroxy-2-phenylacetamide (15e)

White solid, yield 67.3%, mp = 200–202 °C. ^{1}H NMR (600 MHz, DMSO) δ 11.03 (s, 1H), 9.18–8.93 (m, 2H), 7.60–7.53 (m, 1H), 7.46–7.24 (m, 7H), 5.31 (d, J = 8.1 Hz, 1H), 4.42 (d, J = 17.2 Hz, 1H), 4.34–4.26 (m, 2H), 4.06–4.00 (m, 2H), 3.89–3.77 (m, 1H). HRMS (AP-ESI) m/z Calcd for $C_{20}H_{18}BrN_3O_6$ $[M+H]^+$ 476.0379. Found: 476.0461.

5.1.24. 2-(2-(5′-Bromo-2′-oxospiro[[1,3]dioxolane-2,3′-indoline]-1′-yl)acetamido)-*N*-hydroxy-3-methylbutanamide (15f)

White solid, yield 48.4%, mp = 173–174 °C. ^{1}H NMR (600 MHz, DMSO) δ 10.69 (s, 1H), 8.90 (s, 1H), 8.45 (d, J = 8.9 Hz, 1H), 7.60 (d, J = 6.8 Hz, 2H), 6.86 (d, J = 9.0 Hz, 1H), 4.43–4.23 (m, 6H), 3.96 (t, J = 8.3 Hz, 1H), 1.92 (dq, J = 13.8, 6.9 Hz, 1H), 0.85 (dd, J = 11.8, 6.8 Hz, 6H). HRMS (AP-ESI) m/z Calcd for $C_{17}H_{20}BrN_3O_6$ $[M+H]^+$ 442.0535. Found: 442.0602.

5.2. Biological evaluation

5.2.1. In vitro APN inhibition assay

IC_{50} values against APN were determined by using L-leu-*p*-nitroanilide as substrate and Microsomal aminopeptidase from Porcine Kidney Microsomes (Sigma) as enzyme in 50 mM PBS (pH 7.2) or suspension of ES-2 cells in PBS (1×10^5/well). After adding the detected compounds, the solution with various concentrations was incubated with APN at 37 °C for 5 min. Then the solution of substrate was added into the above mixture, which was incubated for another 30 min at 37 °C. The hydrolysis of the substrate was measured by following the change in the absorbance monitored at 405 nm with a plate reader (Varioskan, Thermo, USA).

5.2.2. In vitro HDACs inhibition assay

In vitro HDACs inhibitory activity assay was determined by using Boc-Lys (acetyl)-AMC as substrate and Hela nuclear extract (containing HDAC1, HDAC3, HDAC5 and HDAC8) as enzymes in 15 mM Tris–HCl (PH8.0), at 37 °C. Fist, 10 μL of enzymes solution was added to tested compounds solutions at various concentrations (50 μL) and incubated for 5 min at 37 °C. Then 40 μL of substrate was added and the mixture continued to incubate for another 30 min in the same environment. Finally, 100 μL of developer which containing trypsin and TSA was putted into the mixture. Twenty minutes later, fluorescence intensity was measured at 390 nm excitation and 460 nm emission wavelengths with a microplate reader.

5.2.3. MTT assay

ES-2 cell and MDA-MB-231 cell were grown in RPMI1640 medium with 10% FBS at 37 °C in 5% CO_2 humidified incubator. Cell proliferation was determined by MTT [(3-[4,5-dimethyl-2-thiazolyl]-2,5-diphenyl-2*H*-tetrazolium bromide)] method. In brief, cells were pated in 96-well plates (5000/well) and cultivated for 4 h, and then different concentrations of inhibitors were added. Followed by another 48 h treatment, 1% MTT was added each well. Four hours later, DMSO was added and mixed for 15 min. Finally, the optical density values were monitored at 570 nm.

Acknowledgments

This work was supported by National Science and Technology Specific Projects of China (No. 2009ZX09103-118) and National Nature Science Foundation of China (Nos. 90713041, 30772654 and 21172134).

References and notes

1. Luan, Y.; Xu, W. *Curr. Med. Chem.* **2007**, *14*, 639.
2. Breljak, D.; Gabrilovac, J.; Boranić, M. *Haema* **2003**, *6*, 453.
3. Dixon, J.; Kaklamanis, L.; Turley, H.; Hickson, I. D.; Leek, R. D.; Harris, A. L.; Gatter, K. C. *J. Clin. Pathol.* **1994**, *47*, 43.
4. Raynaud, F.; Bauvois, B.; Gerbaud, P.; Evain-Brion, D. *J. Cell. Physiol.* **1992**, *151*, 378.
5. Piela-Smith, T. H.; Korn, J. H. *Cell. Immunol.* **1995**, *162*, 42.
6. Look, A. T.; Ashmun, R. A.; Shapiro, L. H.; Peiper, S. C. *J. Clin. Invest.* **1989**, *83*, 1299.
7. Inagaki, Y.; Tang, W.; Zhang, L.; Du, G.; Xu, W.; Kokudo, N. *Biosci. Trends* **2010**, *4*, 56.
8. Aoyagi, T.; Yoshida, S.; Nakamura, Y.; Shigihara, Y.; Hamada, M.; Takeuchi, T. *J. Antibiot. (Tokyo)* **1990**, *43*, 143.
9. Repic Lampret, B.; Kidric, J.; Kralj, B.; Vitale, L.; Pokorny, M.; Renko, M. *Arch. Microbiol.* **1999**, *171*, 397.
10. Chung, M. C.; Lee, H. J.; Chun, H. K.; Lee, C. H.; Kim, S. I.; Kho, Y. H. *Biosci. Biotechnol. Biochem.* **1996**, *60*, 898.
11. Ito, K.; Nakajima, Y.; Onohara, Y.; Takeo, M.; Nakashima, K.; Matsubara, F.; Ito, T.; Yoshimoto, T. *J. Biol. Chem.* **2006**, *281*, 33664.
12. Onohara, Y.; Nakajima, Y.; Ito, K.; Xu, Y.; Nakashima, K.; Ito, T.; Yoshimoto, T. *Acta Crystallogr., Sect. F* **2006**, *62*, 699.
13. Addlagatta, A.; Gay, L.; Matthews, B. W. *Proc. Natl. Acad. Sci. U.S.A.* **2006**, *103*, 13339.